Molecular imaging of norepinephrine transporter-expressing tumors: Current status and future prospects

Elin Pauwels[1 ‡], Matthias Van Aerde[1 ‡], Guy Bormans[2], Christophe M. Deroose[1 *]

[1]Nuclear Medicine, University Hospitals Leuven; Nuclear Medicine and Molecular Imaging, Department of Imaging and Pathology, KU Leuven; Leuven, Belgium.
[2]Radiopharmaceutical Research, Department of Pharmacy and Pharmacology, KU Leuven; Leuven, Belgium.

‡ Contributed equally to this work

Short title: Norepinephrine transporter tumor imaging

* Corresponding author: Christophe M Deroose
Address: UZ Leuven, Campus Gasthuisberg
Nucleaire Geneeskunde
Herestraat 49
BE-3000 Leuven
Belgium
Telephone: +32 16 34 37 15
Fax: +32 16 34 37 59
Email: christophe.deroose@uzleuven.be

Conflicts of interest: The authors declare that they have no conflict of interest.

Funding: This research was funded by the project from “Kom op tegen Kanker”: “PET/MR imaging of the norepinephrine transporter and somatostatin receptor in neural crest and neuroendocrine tumors for better radionuclide therapy selection”. Christophe M. Deroose is a Senior Clinical Investigator at Research Foundation – Flanders (FWO).

Abstract

The human norepinephrine transporter (hNET) is a transmembrane protein responsible for reuptake of norepinephrine in presynaptic sympathetic nerve terminals and adrenal chromaffin cells. Neural crest tumors, such as neuroblastoma, paraganglioma and pheochromocytoma often show high hNET expression. Molecular imaging of these tumors can be done using radiolabeled norepinephrine analogs that target hNET. Currently, the most commonly used radiopharmaceutical for hNET imaging is *meta*-[^{123}I]iodobenzylguanidine ([^{123}I]MIBG) and this has been the case since its development several decades ago. The γ-emitter, iodine-123 only allows for planar scintigraphy and SPECT imaging. These modalities typically have a poorer spatial resolution and lower sensitivity than PET. Additional practical disadvantages include the fact that a two-day imaging protocol is required and the need for thyroid blockade. Therefore, several PET alternatives for hNET imaging are actively being explored. This review gives an in-depth overview of the current status and recent developments in clinical trials leading to the next generation of clinical PET ligands for imaging of hNET-expressing tumors.

Key words: norepinephrine transporter, neural crest tumor, MIBG, PET, SPECT

Introduction

The human norepinephrine transporter (hNET) is a transmembrane protein regulating noradrenergic signaling in the peripheral and central autonomous nervous system. Located at the presynaptic membrane of sympathetic nerve terminals and adrenal chromaffin cells, this Na^+/Cl^--dependent monoamine cotransporter is the primary reuptake mechanism for norepinephrine (Figure 1), a catecholamine involved in mood, sleep, behavior, alertness, arousal and regulation of heart rate and blood pressure.[1, 2] The hNET is also expressed by several tumors of neuroendocrine origin, in particular neuroblastoma, pheochromocytoma (PHEO) and paraganglioma (PGL).[3] The fact that these tumor cells are therefore able to specifically take up and store norepinephrine can be exploited in the clinical management of these malignancies both for imaging and therapy.[3] Around 1980, Wieland *et al.*[4] developed radiolabeled *meta*-iodobenzylguanidine (MIBG), a synthetic analog of norepinephrine, for imaging of the adrenal medulla. MIBG is an aryl-alkylguanidine that has an even greater antiadrenergic potency than its two constituents: the benzyl group of bretylium with the guanidine group of guanethidine.[4] As a substrate for the hNET, MIBG is taken up by hNET-expressing tumors as well as normal sympathetically innervated tissues, such as the heart and salivary glands.[5] *In vitro* affinity studies reported 50% inhibitory concentration (IC_{50}) values of 1.2 to 1.7 µM for MIBG binding to the hNET in the human neuroblastoma cell line SK-N-BE(2)C and hNET stably transduced C6 rat glioma cells, respectively.[6, 7] For the past decades iodine-123 and iodine-131-labeled MIBG have been used for imaging and therapy, respectively. Up to now, it is still the most widely used hNET targeting agent.[3]

In this review, we give an overview of the current status of hNET imaging and recent developments leading to the next generation of hNET PET ligands. We will focus on molecular

imaging of hNET-expressing neural crest tumors (neuroblastoma, PHEO and PGL). Although some other tumor types, such as carcinoids (midgut more frequently than foregut tumors), medullary thyroid carcinoma and Merkel cell carcinoma,[8-10] may be able to concentrate MIBG, overall sensitivity is too low for consistent imaging and tracers for other molecular targets, e.g. the somatostatin receptor (SSTR), are recommended.[11, 12]

Neural crest tumors: embryology, epidemiology, genetics and molecular biology

Neural crest cells originate from the ectoderm cell layer. After undergoing an epithelial-mesenchymal transition and delamination, they are able to migrate through the embryo to populate target tissues and differentiate in numerous cell types of different cell lineages.[13] The sympatho-adrenal lineage arises from truncal neural crest cells that migrate ventrally to populate (i) the paravertebral sympathetic ganglia, (ii) the paraganglia and (iii) adrenal medulla where they differentiate into catecholamine-secreting chromaffin cells.[13] Tumors developing from this lineage include neuroblastoma, PHEO, PGL and ganglioneuroma (benign tumors of mature ganglia). The melanocytic lineage gives rise to melanocytes. Malignant transformation results in the most frequent and aggressive neural crest cell tumor, the malignant melanoma.[13] Finally, the Schwann cell lineage also gives rise to melanocytes, along with neurons, fibroblasts, Schwann cells and parasympathetic ganglia. Since tumors from the melanocytic and Schwann cell lineage do not express hNET, they will not be discussed in this review.

Neuroblastoma is a childhood cancer with worldwide incidence rates varying from 3 to 15 per million children under 15 years of age.[14] It represents the most common type of cancer diagnosed in the first year of life,[15] but is only very rarely diagnosed after the age of 15 (0.2% of cancer cases in young people aged 15-19 years).[14] Neuroblastoma is thought to develop from

precursor cells committed to the sympatho-adrenal lineage. They are usually located in the adrenal medulla and paraspinal sympathetic ganglia.[13, 15] Approximately half of the patients show metastatic disease at time of diagnosis, with metastases typically in the regional lymph nodes, bone marrow and bone.[15, 16] Prognosis is highly variable, depending on the risk stratification, with long-term overall survival rates up to 99-100% for children with very-low-risk neuroblastoma and less than 50% for high-risk patients, despite intensive multimodality therapy.[16, 17] The most aggressive tumors exhibit MYCN oncogene amplifications, which is generally associated with poor patient survival, even in localized disease.[16] Differentiation into benign ganglioneuroma and spontaneous regression have also been described, most commonly in infants with stage 4S neuroblastoma.[18] Although the exact mechanisms of spontaneous regression remain unclear, several possibilities have been proposed, such as nerve growth factor depletion, high telomerase activity, immunological mechanisms leading to an anti-tumor immune response and alterations in epigenetic regulation.[18] Since neuroblastoma cells usually show high hNET expression, approximately 90% of the tumors are MIBG avid.[19, 20]

PGL and PHEO are highly vascularized neural crest tumors that arise from autonomic ganglia and chromaffin cells in the adrenal medulla, respectively.[13] The combined estimated age-adjusted incidence is around 6 per million per year, PHEO being four times more common than PGL.[21] Almost all PHEOs and sympathetic PGLs secrete catecholamines, which may result in symptoms of paroxysmal or resistant hypertension, palpitations and perspiration or the patient may even present with arrhythmia, myocardial infarction or stroke.[22, 23] Measurement of free metanephrine (a methylated metabolite of epinephrine) levels in plasma or urinary fractionated metanephrine excretion are the cornerstone for diagnosis, with subsequent imaging to localize the disease sites.[22, 23] Parasympathetic PGLs that are mostly found in the head or neck do not usually produce catecholamines and are diagnosed by their mass effect, or incidentally – as is

also the case for asymptomatic PHEO and sympathetic PGLs – or on the basis of family and germ-line mutation testing.[22, 23] It is estimated that about 40% of PHEO and PGL are hereditary.[24] This increases to 70% in case of multiple PHEOs or the combination of PHEO with a metachronous or synchronous PGL.[25] At least 18 susceptibility genes and 12 genetic syndromes with predisposition of PHEO and PGL have been reported.[23, 24]

Molecular uptake and storage mechanisms

The hNET is a monoamine transporter protein encoded by the SLC6A2 gene, localized on chromosome 16q12.2.[1, 26] In 1995, Pörzgen *et al.*[27] found that the hNET gene spans 45 kb from start to stop codon and consists of 14 exons, disrupted by 13 introns. Three years later, Meyer *et al.*[28] were able to clone and characterize the promotor of the hNET gene. They reported that hNET expression can be seen in direct relation to cyclic adenosine monophosphate (cAMP), because of a cAMP response element located upstream of the core promotor. Only recently, Góral *et al.*[29] extensively studied the crystal structure of the hNET and reconstructed virtual structure models based on their findings. As previously mentioned, the hNET is expressed on the presynaptic plasma membrane of sympathetic neurons and cell membranes of chromaffin cells. As a member of the Na^+/Cl^--dependent cotransporters, like transporters for serotonin, dopamine, glycine and gamma-aminobutyric acid (GABA), it plays a key role in the reuptake of synaptically released norepinephrine and maintaining neurotransmitter homeostasis.[1, 2] As a synthetic analog of norepinephrine, exogenously administered MIBG is transported by the hNET as well. There are three main phases in MIBG handling: uptake, storage and release (Figure 2).[20, 30] Depending on the tumor type, all of the three processes are of varying importance for MIBG-based imaging, as discussed below.

The main uptake pathway (Uptake-1) is an active, specific process mediated by the hNET.[20] As this is a Na^+/Cl^--cotransporter, it is dependent on Na^+/K^+-ATPase to maintain a high extracellular Na^+ concentration. Therefore, it is energy dependent and saturable, requiring a favorable Na^+ gradient as well as a sufficient amount of membrane-bound cotransporters. Furthermore, Uptake-1 is also dependent on pH, temperature, oxygen and vascularity.[20, 31, 32] Consequently, tumors that are located in hyperthermic, hypoxic and nitric oxide depleted environments might be less MIBG-avid than their hNET expression level would allow them to be. Finally, Uptake-1 can be blocked by Na^+/K^+-ATPase inhibitors (ouabain), by competitive inhibition (other catecholamines/analogs) and direct hNET inhibitors (tricyclic antidepressants, such as desipramine (desmethylimipramine), imipramine and clomipramine, and cocaine).[20, 30, 33]

The secondary uptake pathway is a passive, non-specific diffusion through the cell membrane of tumor as well as normal cells.[20, 32] It depends on a concentration gradient of MIBG favorable for inward diffusion. Therefore, it is energy independent and unsaturable, as long as the favorable gradient exists. Furthermore, this uptake is less sensitive and may even increase at elevated temperature.[32] The passive uptake pathway is sometimes referred to as Uptake-2,[20] possibly because the molecular uptake of MIBG was poorly understood before successful cloning of the hNET. However, we advise against the use of this term, as it is also used to refer to an active uptake process in postsynaptic cells of extraneuronal tissue via organic cation transporters (OCTs) (see further).[34, 35] Since Uptake-1 is about 50 times more efficient than its passive counterpart and injected tracer boluses result in low serum concentration, passive MIBG accumulation is considered negligible for molecular imaging purposes.[20, 30] As a result, any pharmacological inhibition of hNET may significantly reduce MIBG uptake.

After uptake through active or passive transmembrane transport, MIBG either remains in the cytoplasm and/or is stored in neurosecretory vesicles or mitochondria.[20] Storage in secretory

vesicles is mediated by vesicular monoamine transporters (VMATs).[36] It is believed that the amount of vesicles is related to the differentiation status and/or degree of maturity: better differentiated and/or more mature cells contain more vesicles.[20, 30] Neuroblastoma, for instance, is a relatively immaturely differentiated tumor type with a limited number of secretory vesicles.[30] As a result, the majority of MIBG remains in the cytoplasm or mitochondria and only a small fraction (about 7%) is stored in neurosecretory vesicles.[20] In contrast, PHEO and PGL are highly differentiated tumors, containing a high number of neurosecretory vesicles.[30] For these tumor types, there is a fairly good correlation between MIBG-avidity and secretory vesicle amount.[30] On the other hand, high MIBG avidity does not imply high neurosecretory capacity, since no clear relationship was observed between uptake of MIBG and the plasma and urinary concentration of catecholamines and their metabolites.[30] Hence MIBG-avidity is only an indicator for the amount of catecholamines stored in a particular tumor.

Some studies suggest an important role of VMAT in retention of MIBG, since long-term retention of MIBG was only observed in tissues with a high level of VMAT expression and MIBG accumulation was effectively reduced by reserpine, a VMAT antagonist.[36] On the other hand, in contrast to norepinephrine, which is rapidly degraded when it remains intracellularly, MIBG is enzymatically stable and does not require storage into vesicles for retention.[37] Especially in the case of neuroblastoma, VMAT expression is likely of minor importance compared to hNET expression for MIBG avidity.[20]

It is thought that extended MIBG retention is possible due to the dynamic equilibrium of catecholamine release and reuptake.[38] Reuptake, mediated by the hNET, is dependent on optimal working conditions. If these conditions are compromised (e.g. high temperature), it is believed that hNET could reverse and MIBG cotransport could occur to the extracellular space.[20] For optimal diagnostics, further research on stimulating (re)uptake and storage and inhibiting efflux is of high interest.

hNET enhancers

Even though the majority of neuroblastomas are [^{123}I]MIBG-avid, the mean objective response rate to [^{131}I]MIBG therapy is only about 30% in clinical trials.[39] Therefore, strategies to improve therapeutic outcome have been explored. Although controversial, several compounds have been suggested as possible enhancers of the hNET, effectively increasing potential MIBG and catecholamine uptake when administered together.[40-45]

Corticosterone is one such compound.[40, 41] Judging by scintigraphic imaging patterns of MIBG uptake in several cell types, a fraction of the administered activity is concentrated in cells expressing OCTs (also sometimes referred to as Uptake-2) that are located in several normal tissues, such as the liver (hepatocytes), intestine (epithelial cells), heart (myocytes), kidney (tubulus cells and cortex) and central nervous system (glia, neurons).[40] For imaging, it is of interest to keep this fraction to a minimum, as these cells may compete for MIBG uptake at the expense of neural crest tumor cells. It was shown that corticosterone, which acts as an inhibitor of OCTs, significantly reduces MIBG uptake in OCT expressing cells.[40] This was also the case for clinically approved corticosteroids like hydrocortisone and prednisolone.[41] Thus, administering a single intravenous (IV) dose of hydrocortisone or prednisolone prior to [^{123}I]MIBG scintigraphy or [^{131}I]MIBG therapy might improve specificity and reduce radiation dose to non-target organs, respectively.[41] Further clinical studies are necessary to support this hypothesis, since clinical data is limited to a single case study, where normal heart and liver uptake were reduced in comparison to patients not pretreated with hydrocortisone.[41]

Another example is the naturally occurring compound hydroxytyrosol. In rat pheochromocytoma PC12 cells, hydroxytyrosol potently increased hNET activity within minutes.[42] The exact mechanism remains unknown, but is thought to be related to the strong

antioxidant properties of hydroxytyrosol. Neural crest tumors like PHEO are known to excrete massive amounts of norepinephrine, hereby inducing oxygen free radical formation resulting in oxidative stress.[42]

Vorinostat, a histone deacetylase (HDAC) inhibitor that causes transcriptional activation of several genes, including those responsible for hNET expression, was also found to increase hNET expression in neuroblastoma cells, causing a dose-dependent increase in MIBG uptake.[43] Moreover, it has radiosensitizing effects on neuroblastoma cells as well.[46] In a phase I clinical trial in 27 neuroblastoma patients, the combination of [^{131}I]MIBG with vorinostat was found tolerable.[44] Evaluation of overall response rates is subject of an ongoing randomized phase II trial comparing [^{131}I]MIBG alone to [^{131}I]MIBG/vorinostat and [^{131}I]MIBG/vincristine/irinotecan (clinicaltrials.gov identifier: NCT02035137).

Pretreatment with traditional chemotherapeutic agents, such as doxorubicin and cisplatin, has also been reported to increase hNET expression, thereby improving MIBG uptake.[20, 45] Furthermore, topoisomerase I inhibitors, such as topotecan may improve accumulation of MIBG, apart from acting as a radiosensitizer.[47] In a recent retrospective clinical trial in 10 neuroblastoma patients, the combination of topotecan and [^{131}I]MIBG therapy was found to be well tolerated and effective with high response rates.[48] Further studies in larger patient groups are ongoing (NCT03165292).

Also several signaling pathways involved in regulation of hNET expression, including protein kinase C (PKC), calcium/calmodulin dependent protein kinase (CaMK), mitogen activated protein kinase (MAPK) and phosphatidyl inositol-3 kinase (PI3K) may be further explored to enhance hNET expression.[20]

Interfering drugs

Many (classes of) drugs are known to, or highly likely to, interfere with uptake and/or storage of MIBG, such as labetalol, tricyclic antidepressants and sympathomimetics (e.g. vasoconstrictors in nasal sprays).[5, 33, 49] Therefore, it is recommended that these drugs are interrupted prior to MIBG administration until after imaging. The withdrawal time should be typically four to five biological half-lives.[5, 33] However, for labetalol for instance, a longer withdrawal time of seven up to ten days is recommended.[5, 50]

In the 2010 EANM guidelines for [$^{123/131}$I]MIBG tumor imaging, an extensive list was published with interfering drugs and recommended withdrawal times.[49] However, it is important to realize that the effect on MIBG uptake of many of these drugs has never been actually tested.[25, 33] Moreover, although most of these listed medications have a connection with MIBG uptake and/or storage pathways, their mechanism of action does not always result in reduced MIBG uptake and/or storage. Beta agonists, such as salbutamol, for example are typically listed as medication that interferes with MIBG handling. However, these drugs act on post-synaptic beta-2 receptors and therefore have no effect on presynaptic neurons.[33] As a result, their withdrawal is not required. Also calcium antagonists are often listed for withdrawal, although there is no definite proof and their effect (if any) is on MIBG release, not uptake.[33] Withdrawal of calcium antagonists is therefore not necessary. An updated list of the classes of interfering drugs was recently published in the EANM guidelines for neuroblastoma imaging.[5]

Reporter gene imaging

Reporter gene imaging is a method of molecular genetics research.[51] It employs both molecular biology and genetics to study gene expression, signal transduction, receptor activation, protein-protein interaction and several other molecular events in a non-invasive way.[51] A reporter gene is a gene that expresses a protein that can be readily detected. For imaging genes, the detection

is done by a non-invasive imaging modality which can be qualitative or quantitative. The signal strength within the images should correlate with the expression level of the reporter gene.

The hNET gene has been suggested as a useful reporter gene.[37, 52, 53] When coupled to a specific promoter, transcription and translation in cells where this promoter is active will lead to significant hNET expression. The density of this transmembrane transporter is dependent on the transcription rate dictated by the regulatory sequences to which the hNET reporter gene was coupled. Preclinical studies have shown that hNET is suitable for molecular imaging, especially with [^{124}I]MIBG positron emission tomography (PET) and [^{123}I]MIBG single photon emission computed tomography (SPECT).[37, 52, 53] The human origin of hNET is an advantage from an immunological point of view compared to other PET reporter genes of viral or mammalian origin and hNET directed radionuclide therapy can be used as a suicide mechanism, similar to the SSTR.[54]

A theoretical advantage of hNET imaging is the plasma membrane location of the protein, which allows an interaction with its substrate while it is still extracellular and hence the substrate does not need to diffuse through the cell membrane nor is dependent on transport by another transporter than hNET. Another advantage is signal amplification: one protein unit of hNET can transport many molecules of the substrate, which is not the case for instance in a receptor/ligand system.[55] This explains why very high target to non-target ratios have been obtained (≈300 fold) in rodent models.[53] There is a potential for MIBG imaging applications in other applications than tumors inherently expressing hNET.

Current status in hNET imaging: *meta*-iodobenzylguanidine

In 1981, not long after the development of MIBG,[4] hNET imaging was first performed in eight PHEO patients using [^{131}I]MIBG (Figure 1).[56] A few years later, the first reports on successful

[^{131}I]MIBG imaging in neuroblastoma, carcinoid tumors, PGL and other neuroendocrine tumors were published.[8, 10, 57] Iodine-131 decays with a half-life of 8.0 days via β^- emission (606 keV, 89% intensity) to excited states of xenon-131, immediately followed by γ emissions (364 keV, 81% intensity) (Table 1). As a β^--emitter with a long half-life, iodine-131 is not a suitable radioisotope for imaging purposes. Moreover, its high-energy γ-rays result in relatively low spatial resolution of the resulting images. Therefore, diagnostic [^{131}I]MIBG imaging is now only indicated when [^{131}I]MIBG therapy is considered and [^{123}I]MIBG is not available.[5] [^{131}I]MIBG therapy has been used for decades and is still a validated therapeutic option in the treatment of inoperable neural crest tumors.[3, 58]

Iodine-123 decays through electron capture to excited levels of tellurium-123, immediately followed by γ emissions (159 keV, 83% intensity) with a half-life of 13.2 hours (Table 1). Although [^{123}I]MIBG is more costly than [^{131}I]MIBG, it has largely replaced the latter and is now strongly preferred for diagnostic use.[3, 25, 59] The lower radiation dose allows for a higher activity to be administered, which in combination with the lower energy of the emitted γ-rays and thus higher spatial resolution, results in superior image quality compared to [^{131}I]MIBG scintigraphy.[25] Consequently, [^{123}I]MIBG has a higher sensitivity than diagnostic [^{131}I]MIBG imaging.[5, 60] Furthermore, the recommended interval between tracer injection and imaging is shorter for [^{123}I]MIBG (24 h) than for [^{131}I]MIBG (48-72 h).[25]

In Europe, [^{123}I]MIBG has been commercially available since the mid-nineties, whereas in the USA it was only approved by the Food and Drug Administration (FDA) in 2008.[59] [^{123}I]MIBG scintigraphy and SPECT has been the gold standard for hNET imaging in neural crest tumors for nearly four consecutive decades.

After IV administration, [^{123}I]MIBG is rapidly cleared from the blood and accumulated in sympathetically innervated tissues, with especially prolonged retention in the highly innervated tissues, such as the heart (myocardium), adrenal medulla and salivary glands.[61] In the heart, the

highest uptake is reached after 2-3 hours, whereas in tumors, maximum accumulation is achieved after 24-96 hours.[61] Other organs with normal uptake include the liver, nasopharynx, unblocked thyroid, bowel, bladder (due to excretion), lungs, brown adipose tissue and occasionally the lacrimal glands.[5, 25] [^{123}I]MIBG is mainly excreted unaltered by the kidneys (about 50% within 24 h; about 90% after 4 days).[61] Part of the tracer may also be excreted via the bowel [5], and high intestinal activity may therefore be observed in some cases.[25] In the adrenal glands, symmetric [^{123}I]MIBG uptake, which is lower or equal to liver uptake is considered normal.[25] However, in patients with unilateral adrenalectomy, the remaining adrenal may show more prominent [^{123}I]MIBG uptake due hyperplasia, which is considered physiological.[5] As there is low bone and bone marrow uptake, the spine is typically visualized as a photopenic stripe on planar posterior images. An example of [^{123}I]MIBG scintigraphy in a PGL patient is shown in Figure 3.

For neuroblastoma patients, the sensitivity and specificity have been estimated at 88%–97% and 83%, respectively.[33, 62] For PHEO and PGL combined, reported sensitivity and specificity both lie in the range of 82%–100%.[25, 33, 63, 64] Overall, sensitivity for PGL was lower than for PHEO (67%–100% vs. 87%–90%).[63] However, in all these studies the reference standard was a combination of histopathology, blood and urine catecholamine measurements, recent conventional imaging (compute tomography (CT), MRI and scintigraphy) and clinical follow-up. Therefore, sensitivity and specificity values were driven by the fact that [^{123}I]MIBG itself was the best molecular imaging diagnostic tool available at that time. With current improvements of PET radiopharmaceuticals, PET cameras and radiological techniques, it is becoming clear that [^{123}I]MIBG sensitivity, and to a lesser extent specificity, could have been overestimated in the past. In a recent systematic review and meta-analysis, the diagnostic accuracy of [$^{123/131}$I]MIBG scintigraphy and PET(/CT), using a range of tracers, in neuroblastoma were evaluated and compared.[65] The authors found an overall sensitivity of 79%

and 89% for [$^{123/131}$I]MIBG and PET(/CT) using a range of tracers in neuroblastoma imaging, respectively. This difference could be mainly attributed to a higher sensitivity for PET(/CT) compared to [$^{123/131}$I]MIBG scintigraphy in lesion-based analyses (90% vs. 69%). Sensitivities on the patient level were comparable (82% for PET/(CT) vs. 87% for [$^{123/131}$I]MIBG). [$^{123/131}$I]MIBG showed better specificity than PET/(CT), with an overall specificity of 84% for [$^{123/131}$I] MIBG and 71% for PET(/CT).[65] However, this finding may result from the fact that several studies with [^{18}F]FDG, which typically has a low specificity, were included in the meta-analysis as well. For PHEO and PGL, the reported sensitivities for [^{123}I]MIBG imaging in studies where PET ligands were evaluated lie between 50% and 85%.[25, 59, 66-69] In *SDHB*-associated PHEO and PGL, [^{123}I]MIBG scintigraphy frequently shows false-negative results, especially on a region/lesion level, and is therefore not recommended as first choice examination.[25, 66, 70, 71] This is also the case for metastatic PHEO and PGL.[25, 66, 72] Furthermore, in head and neck PGL, sensitivity of [^{123}I]MIBG scintigraphy is also below that of other imaging modalities,[73] and [^{68}Ga]Ga-DOTA-somatostatin analog (SSA) PET is recommended instead.[25, 74] Nevertheless, [^{123}I]MIBG is still the most widely used radiopharmaceutical for hNET imaging and remains the diagnostic agent of choice when [^{131}I]MIBG therapy is considered.

As [$^{123/131}$I]MIBG scintigraphy has been the most commonly used molecular imaging examination for neuroblastoma for several decades, semi-quantitative scoring systems have been developed to provide an objective and standardized assessment of the disease load that correlate with survival and treatment response.[5] The most widely used and internationally accepted and validated systems are the Curie scoring system and the International Society of Paediatric Oncology Europe Neuroblastoma (SIOPEN) scoring system (Table 2).[5, 75, 76] Both are scored on planar [$^{123/131}$I]MIBG images. The Curie score divides the skeleton into nine areas: skull (1), cervical and thoracic spine (2), ribs and sternum (3), lumbar and sacral spine (4),

pelvis (5), upper arms (6), forearms and hands (7), thighs (8) and legs and feet (9).[75] Each area is assigned a score according to [$^{123/131}$I]MIBG uptake as follows: 0, no site of involvement; 1, one site of involvement; 2, more than one site of involvement; 3, involvement of > 50% of the area. Most commonly, a general, non-skeletal category is added as a tenth segment to the nine skeletal segments to take into account overall soft tissue involvement. This is often referred to as the "modified Curie score". The soft tissue segment is assigned a score of 0 for no involvement, 1 for a single soft tissue lesion, 2 for two or more soft tissue lesions and 3 for soft tissue lesions occupying an area of more than 50% of the chest or abdomen as evaluated on planar [$^{123/131}$I]MIBG images.[77] As such, the maximum score is 30. The SIOPEN score divides the skeleton in 12 anatomical body segments: skull (1), thoracic cage (2), proximal right upper limb (3), proximal left upper limb (4), distal right upper limb (5), distal left upper limb (6), spine (7), pelvis (8), proximal right lower limb (9), proximal left lower limb (9), distal right lower limb (11) and distal left lower limb (12).[76] Each segment is assigned a score according to [$^{123/131}$I]MIBG involvement as follows: 0, no abnormality; 1, one discrete focus; 2, two discrete foci; 3, three discrete foci; 4, more than three discrete foci or diffuse involvement < 50% of the segment; 5, diffuse involvement 50-95% of the segment; 6, uniform, diffuse whole bone involvement.[76] As such, the maximum score is 72. Importantly, these scoring systems have a prognostic value that can help guide treatment decisions.[78] The modified Curie score and SIOPEN score and their prognostic value have been compared in a retrospective study analyzing 147 [^{123}I]MIBG scans in 58 neuroblastoma patients, aged 1 year or older.[79] They were found to be equally reliable and predictive. An optimal cutoff point of 2 or less for the Curie score and 4 or less for the SIOPEN score at diagnosis, correlating with better 5-year event-free survival (EFS) and overall survival (OS), were identified.[79] Survival rates are shown in Table 2.

Active research and future prospects in hNET imaging

Conventional nuclear medicine (planar scintigraphy and SPECT) has several disadvantages compared to PET. It has a lower sensitivity (counts per activity) and spatial resolution which may compromise diagnostic sensitivity. Moreover, image quantification is far more challenging with SPECT than with PET. Additionally, only PET ligands allow for simultaneous MR imaging by means of a hybrid PET/MR scanner. This could be especially useful in pediatric patients.[3] Finally, the use of iodine-123 (or iodine-131) has some additional practical drawbacks such as a multi-day imaging protocol and the need for thyroid blocking.[5] Therefore, several PET alternatives for hNET imaging have been developed and are actively being explored. Here, we provide an overview of current findings from clinical trials.

[^{124}I]MIBG

The PET alternative which is most similar to [^{123}]IMIBG is [^{124}I]MIBG (Figure 1), with identical chemical properties. Iodine-124 decays with a half-life of 4.2 days to tellurium-124, predominantly through electron capture (77%), and to a lesser extent through β^+ decay (mean energy 820 keV, 23%). It has a complicated decay scheme, involving several high-energy γ-rays, the majority (63%) with an energy of 603 keV, but with energies as high as 1.7 MeV (11%) (Table 1). These high-energy emissions may compromise image quality and contribute to patient and personnel radiation exposure.[3] Furthermore, broad applicability of [^{124}I]MIBG is restricted by high production cost, limited availability and the need for multi-day imaging.[3] Nevertheless, a few small clinical case studies proved that [^{124}I]MIBG imaging is feasible in neuroblastoma and PHEO or PGL patients, but large scale evidence for validated clinical use is lacking.[80, 81] Current evidence suggests dosimetry prior to [^{131}I]MIBG as its main use,[82-84] although this can also be performed with [^{123}I]MIBG. The concept of pretreatment planning is

that a radiopharmaceutical, which acts as a proxy for the therapeutic radiopharmaceutical, is used to predict the pharmacokinetics of the therapeutic radiopharmaceutical.[84] Since the half-life of iodine-124 is in the order of magnitude of the half-life of iodine-131 (4.2 vs. 8.0 days, respectively), and thus significantly longer than that of iodine-123 (13.2 hours), [^{124}I]MIBG is theoretically more suitable than [^{123}I]MIBG for pretreatment dosimetry. The complex decay scheme of [^{124}I]MIBG with low positron yield still offers reasonable image quality and quantification for diagnostics and dosimetry, respectively.[82] Other strategies to determine injected activity are based on patient body weight, iodine-131 residence in previous [^{131}I]MIBG studies or [^{123}I]MIBG planar and/or SPECT/CT imaging.[82]

Reporter gene imaging of hNET with [^{124}I]MIBG has also been described in literature, albeit only in preclinical studies.[52, 53]

[^{18}F]MFBG

In 1994, Garg *et al.*[85] developed a promising fluorine-18-labeled analog of MIBG, *meta*-[^{18}F]fluorobenzylguanidine ([^{18}F]MFBG), to tackle the limitations associated with the use of [^{123}I]MIBG in clinical practice (Figure 1). Fluorine-18 is a β^+-emitter (mean energy 250 keV, 99.8%) that decays with a half-life of 109.8 minutes to oxygen-18 (Table 1). It is by far the most commonly used radionuclide for PET imaging in clinical practice. It can be produced with a cyclotron and its half-life is long enough to allow centralized production and transport to distant PET centers without an on-site cyclotron.[86] Relatively recently, novel chemical approaches to introduce fluorine-18 in a non-activated aromatic ring were developed allowing reliable and robust radiosynthesis of clinical grade [^{18}F]MFBG.[87, 88]

In vitro affinity studies found IC_{50} values of 3 to 5 µM for MFBG binding to the hNET, which are in line with those for MIBG.[6, 7] Zhang *et al.*[6, 7] also performed *in vivo* biodistribution and imaging studies in mice bearing xenografts with high levels of hNET expression. [^{18}F]MFBG

showed a rapid and high accumulation in the xenografts, salivary glands and bladder, and was quickly cleared from plasma and excreted with urine. Tumor uptake tended to plateau at one hour post-injection, with further increasing tumor-to-background ratios (TBGs) due to rapid whole-body clearance of radioactivity through the urinary system. In comparison, TBGs at one and four hours after injection for [^{123}I]MIBG were lower than for [^{18}F]MFBG, but significantly improved 24 hours after injection.[6] As a more hydrophobic ligand, [^{123}I]MIBG undergoes not only renal clearance, but also hepatobiliary clearance, resulting in greater retention in the liver and gall bladder and more intestinal activity than the more hydrophilic [^{18}F]MFBG.[7] This could lead to better differentiation of abdominal tumors with [^{18}F]MFBG, especially with the added superiority of PET imaging.

Following these promising preclinical results, Pandit-Taskar *et al.*[89] performed a first-in-human PET/CT study with in five patients with confirmed neuroblastoma and five patients with confirmed PGL/PHEO. [^{18}F]MFBG was well tolerated and showed an excellent safety profile. The mean effective dose was 0.023 ± 0.012 mSv/MBq, which is comparable to that of ^{123}I-MIBG (0.013 mSv/MBq for adults and 0.037 mSv/MBq for 5 year olds[49]). The overall biodistribution with [^{18}F]MFBG was similar to that of [^{123}I]MIBG, with more favorable rapid clearance from blood pool and organs. Excellent lesion targeting was observed with high tumor uptake and TBGs. [^{18}F]MFBG was able to visualize all lesions seen on [^{123}I]MIBG scans obtained within 4 weeks prior to the study scans. Moreover, additional lesions were detected in all patients (103 at 30–60 minutes and 122 at 3–4 hours after [^{18}F]MFBG injection vs. 63 with [^{123}I]MIBG). The authors suggest that the optimal time point for imaging would be 1-2 h post injection, since the tumor-to-background ratios are highest at that time point and the difference in detected number of lesions was not statistically significant between 1-2h and 3-4h.[89]

Currently, [^{18}F]MFBG is being further validated for clinical use in two ongoing prospective trials (clinicaltrials.gov identifier: NCT02348749, NCT04258592).[90] A head-to-head

comparison of [^{123}I]MIBG scintigraphy and [^{18}F]MFBG PET is shown in Figure 3 (patient data from NCT04258592).

[^{11}C]HED

Carbon-11-*meta*-hydroxyephedrine ([^{11}C]HED) is a norepinephrine analog that was developed to image the sympathetic nervous system (Figure 1).[91] Carbon-11 decays with a half-life of 20.4 minutes via β^+-emission (mean energy 386 keV, 99.77%), and a negligible fraction via electron capture (0.23%), to boron-11 (Table 1). Due to its short half-life, its usage requires a nearby cyclotron. As a synthetic norepinephrine analog, HED is taken up by cells expressing the hNET. Similarly to MIBG and unlike norepinephrine, HED is not degraded intracellularly.[91] Even though [^{11}C]HED was developed for cardiac applications and is currently mainly used for these purposes, several studies have shown that it is also suitable for hNET imaging in neural crest tumors.[92-97] In a mixed series of 14 neural crest tumor patients (6 neuroblastoma, 1 ganglioneuroblastoma, 5 PHEO and 2 PGL), [^{11}C]HED showed a higher lesion detection rate (80/81) than [^{123}I]MIBG (75/81).[92] However, one large abdominal neuroblastoma lesion due to local relapse was only seen with [^{123}I]MIBG, which had a clear impact on clinical management. Moreover, 10 of 14 soft tissue lesions in neuroblastoma patients showed higher uptake with [^{123}I]MIBG than with [^{11}C]HED, as visually assessed, whereas in the whole patient group, this was only the case for 14 out of 62 soft tissue lesions (30 showed equal uptake with both tracers).[92] In a small cohort of 7 neuroblastoma patients, tumor uptake was seen within 5 minutes after injection of [^{11}C]HED, but also prominent liver uptake was observed.[94] Consequently, abdominal lesions in two patients were better detected with [^{123}I]MIBG. For PHEO, high sensitivities between 90% and 100% with [^{11}C]HED have been reported in several small patient series.[93, 95, 96] In these studies, the two false-negative results with [^{11}C]HED were also negative with MIBG scintigraphy.[95, 96] Finally, a large retrospective study in 134 patients

with suspected or confirmed PHEO or PGL who underwent [^{11}C]HED PET imaging, reported a sensitivity of 91% and specificity of 100%.[97] However, in multiple endocrine neoplasia type II patients, sensitivity of [^{11}C]HED PET was lower (73%).[97]

Further prospective research in larger patient series may prove worthwhile, but the necessity of an on-site cyclotron and the limited amount of patients that can be scanned per production batch, will hamper the widespread clinical implementation of [^{11}C]HED PET.

[^{18}F]FDA

6-[^{18}F]fluorodopamine ([^{18}F]FDA) is a positron-emitting analog of dopamine, developed at the National Institutes of Health (NIH) as a sympathoneuronal imaging agent.[98] Dopamine plays a key role in the central nervous system as a catecholamine neurotransmitter. It is a somewhat better substrate for the hNET than norepinephrine itself.[34] [^{18}F]FDA can therefore be actively taken up by hNET-expressing tumors. It is further transported by VMAT into secretory vesicles, where it is converted to 6-fluoronephrine.[34] Alternatively and contrary to MIBG and HED, it can also be metabolized by monoamine oxidase (MAO).[34]

Several clinical studies have demonstrated the potential of [^{18}F]FDA imaging in PHEO and PGL in well over 300 patients with reported sensitivities between 88% and 100% on the patient level.[66, 67, 69, 70, 98-101] The largest prospective trial by Timmers *et al.*[67] in 99 patients with known or suspected PHEO, the sensitivity of [^{18}F]FDA was 78% for non-metastatic disease and 97% for detecting metastases in a patient-based analysis. The specificity of [^{18}F]FDA PET was 90%. Most patients also underwent [$^{123/131}$I]MIBG scintigraphy within three months prior or after [^{18}F]FDA PET. The sensitivity of [$^{123/131}$I]MIBG scintigraphy was equal to [^{18}F]FDA PET for non-metastatic disease (78% [^{123}I]MIBG only and 76% pooled [$^{123/131}$I]MIBG), but lower for detecting metastatic disease (85% [^{123}I]MIBG only and 65% pooled [$^{123/131}$I]MIBG).[67] Timmers *et al.*[66] also performed a large prospective observational trial in 53 patients with known or

suspected PGL. All patients underwent [^{18}F]FDA PET and 50 patients underwent [^{123}I]MIBG as well. The sensitivity for detecting non-metastatic disease was 78% for both tracers. In metastatic [^{18}F]FDA PET performed better than [^{123}I]MIBG scintigraphy with a sensitivity of 76% compared to 57% in a region-based analysis (neck, thorax, abdomen/pelvis).[66]

Notwithstanding these promising results, the limited availability of [^{18}F]FDA restricts its widespread use in clinical practice. Regarding neuroblastoma, evidence from clinical studies is still lacking, but a phase one trial is currently ongoing (clinicaltrials.gov identifier: NCT03541720).

Other hNET PET ligands

In 2014, a case report was published comparing [^{18}F]-fluoropropylbenzylguanidine ([^{18}F]FPBG) PET/CT with [^{123}I]MIBG scintigraphy in a 14-year-old neuroblastoma patient.[102] [^{18}F]FPBG showed prominent uptake in the liver, similar to [^{123}I]MIBG, but also in the small intestine and cartilage growth plate, higher than [^{123}I]MIBG. A focal neuroblastoma lesions was readily observed with [^{18}F]FPBG PET that could not be detected with [^{123}I]MIBG scintigraphy (only planar images were made).[102] To our knowledge, [^{18}F]FPBG has not been further studied in clinical trials.

When [^{18}F]MFBG was developed in 1994, Garg *et al.*[85] simultaneously developed *para*-[^{18}F]fluorobenzylguanidine ([^{18}F]PFBG). Since [^{18}F]MFBG gave better preclinical results than [^{18}F]PFBG, up to now, only [^{18}F]MFBG underwent clinical translation, although radiosynthesis of [^{18}F]PFBG was more convenient.[7, 85, 89] Nevertheless, [^{18}F]PFBG has recently been further evaluated in a preclinical trial in three monkeys.[103]

In 1994, also another compound was suggested as a potential MIBG analog for hNET PET imaging, 4-[^{18}F]fluoro-3-iodobenzylguanidine ([^{18}F]FIBG).[104] Further preclinical studies, showed that [^{18}F]FIBG is an excellent analog of MIBG,[105] with tumor uptake and detectability

in mice bearing the rat pheochromocytoma cell line PC-12 similar to MIBG.[106] However, due to the complex radiolabeling procedures and low production yield, further optimization of radiosynthesis is warranted before clinical translation.[106] FIBG can also be labeled with iodine-131 allowing for radionuclide therapy. Interestingly, [^{131}I]FIBG showed a higher and longer retention in tumors of PC12 bearing mice than [^{125}I]MIBG and a better therapeutic effect than [^{131}I]MIBG.[106] Further studies in other, more relevant clinical models are required, prior to clinical translation.

Several other hNET PET radiopharmaceuticals have been developed specifically for cardiac applications, but could prove to be useful for hNET tumor imaging in the future as well. An example that already underwent a first clinical translation is N-[3-bromo-4-(3-[^{18}F]fluoro-propoxy)-benzyl]-guanidine or [^{18}F]LMI1195.[107] This PET tracer is being used for imaging and quantifying sympathetic denervation in an ongoing clinical trial (clinicaltrials.gov identifier: NCT03493516). A preclinical trial in MENX-affected rats showed high and specific uptake of [^{18}F]LMI1195 in PHEO.[108] To our knowledge, clinical trials with [^{18}F]LMI1195 in hNET-expressing tumors have not yet been performed. Two other promising hNET PET tracers that have been developed for assessment of cardiac sympathetic denervation and recently underwent first-in-human evaluation are the [^{18}F]fluorohydroxyphenethylguanidines, 4-[18F]fluoro-meta-hydroxyphenethylguanidine ([^{18}F]4F-MHPG) and 3-[18F]fluoro-para-hydroxyphenethylguanidine ([^{18}F]3F-PHPG).[109] Both preclinical and clinical evaluation in hNET-expressing tumors have yet to be performed.

Other PET tracers for neural crest tumor imaging

6-[^{18}F]fluoro-L-dihydroxyphenylalanine ([^{18}F]FDOPA) is an analog of DOPA, the precursor of dopamine, norepinephrine and epinephrine.[5] It is taken up in cells by L-type amino acid

transporters (LATs), predominantly LAT1, and therefore does not directly target hNET.[3, 25] After uptake it is rapidly converted to [^{18}F]FDA by aromatic L-amino acid decarboxylase enzymes.[25] [^{18}F]FDOPA is commercially available, but in the USA, it has not been approved and its use is therefore restricted to clinical studies.[25] In Europe, it is authorized for use in certain countries.

A meta-analysis of 11 studies in 275 PGL patients evaluating the diagnostic performance of [^{18}F]FDOPA, reported a pooled sensitivity of 91% [95% confidence interval (CI) 87–94%] on the patient level and 79% [95% CI 76–81%] on lesion level.[110] Pooled specificities were 95% [95% CI 86–99%] and 95% [95% CI 84–99%] in a patient-based and lesion-based analysis, respectively. Fiebrich *et al.*[68] compared the diagnostic performance of [^{18}F]FDOPA PET with [^{123}I]MIBG scintigraphy (planar images and SPECT) in a prospective trial in 48 patients with catecholamine excess. Forty patients were eventually diagnosed with PHEO, two with PGL, two with adrenal hyperplasia and in three diagnosis remained unknown. [^{18}F]FDOPA PET showed a superior sensitivity compared to [^{123}I]MIBG scintigraphy, both on a per-patient basis and per-lesion basis (90% vs. 65% and 73% vs. 48%, respectively).[68] According to the current guidelines of the European Association of Nuclear Medicine (EANM), [^{18}F]FDOPA PET and [^{123}I]MIBG scintigraphy are both recommended as first-line molecular imaging modalities for sporadic, non-metastatic PHEO, but in case of inherited PHEO, [^{18}F]FDOPA should be preferred (except in *SDHx*-associated tumors where [^{68}Ga]Ga-DOTA-SSA are first choice).[25]

[^{18}F]FDOPA PET imaging can also be used for neuroblastoma, but current evidence in clinical trials is less extensive than for PHEO or PGL.[3, 5] In a prospective trial in 28 patients with stage 3 and 4 neuroblastoma, [^{18}F]FDOPA PET was compared with [^{123}I]MIBG scintigraphy (planar images and SPECT).[111] [^{18}F]FDOPA PET outperformed [^{123}I]MIBG scintigraphy with sensitivities of 95% versus 68% and 90% versus 57% on patient and lesion level, respectively. Recently, Piccardo *et al.*[112] published the results of a prospective trial in 18 children with

neuroblastoma at onset to evaluate the role of [^{18}F]FDOPA PET in initial staging and assessment of response to chemotherapy, compared to [^{123}I]MIBG scintigraphy. Also in this patient cohort, a superior performance of [^{18}F]FDOPA PET was observed.[112] Larger, prospective trials are warranted to validate the role of [^{18}F]FDOPA PET in the management of neuroblastoma patients.[3]

As the most widely used PET radiopharmaceutical in clinical practice, 2-[^{18}F]fluoro-2-deoxy-D-glucose ([^{18}F]FDG) is also used in neural crest tumor imaging.[5, 25] The sensitivity of [^{18}F]FDG PET for PHEO and PGL is overall high, between 76 and 100%, but, as in other malignancies, specificity is low.[25, 59, 113] In metastatic disease, [^{18}F]FDG has high diagnostic potential, especially in case of *SDHB*-associated PHEO or PGL.[66, 70, 101, 113, 114] According to the EANM guidelines, it is recommended as second choice examination (after [^{68}Ga]Ga-DOTA-SSA) in case of extra-adrenal sympathetic, multifocal, metastatic and/or *SDHx*-associated PHEO or PGL.[25] Also for neuroblastoma imaging, [^{18}F]FDG PET is considered as a second-line imaging modality as it is less specific than [^{123}I]MIBG scintigraphy.[5] As such, it is indicated for staging, evaluation of treatment response, evaluation of post-therapeutic changes and follow-up.[5]

Finally, also [^{68}Ga]Ga-DOTA-SSAs are used for PET imaging of neural crest tumors as these often also express the SSTR.[5, 25, 86] The tracers currently used in clinical practice are [^{68}Ga]Ga-DOTA-Tyr^{3}-octreotate ([^{68}Ga]Ga-DOTATATE), [^{68}Ga]Ga-DOTA-Tyr^{3}-octreotide ([^{68}Ga]Ga-DOTATOC) and [^{68}Ga]Ga-DOTA-1-NaI^{3}-octreotide ([^{68}Ga]Ga-DOTANOC).[86] In a recent systematic review and meta-analysis evaluating the diagnostic performance of [^{68}Ga]Ga-DOTA-SSA PET in patients with PHEO and PGL, the pooled per-lesion detection rate was 93% [95% CI 91%–95%], which was significantly higher than that of [$^{123/131}$I]MIBG

scintigraphy (38% [95% CI 20%–59%]), [^{18}F]FDOPA PET (80% [95% CI 69%–88%]) and [^{18}F]FDG PET (74% [95% CI 46%–91%]) ($p < 0.001$ for all).[115] According to the current EANM guidelines, [^{68}Ga]Ga-DOTA-SSA PET is considered the first choice investigation for head and neck PGL and extra-adrenal sympathetic, multifocal, metastatic and/or *SDHx*-associated PHEO or PGL.[25] Evidence regarding imaging in neuroblastoma patients is limited, although clinical experience suggests a higher sensitivity for [^{68}Ga]Ga-DOTA-SSA PET compared with [^{123}I]MIBG scintigraphy.[5] Furthermore, [^{68}Ga]Ga-DOTA-SSA PET is indicated when peptide receptor radionuclide therapy is considered.[5]

Conclusion

[^{123}I]MIBG has been the go-to radiopharmaceutical for imaging hNET-expressing tumors since its development several decades ago and still holds up today offering decent diagnostic sensitivity and wide availability. hNET imaging is mandatory if radionuclide therapy targeting hNET is considered in patients with inoperable neural crest tumors. It is clear that the role of PET imaging in neural crest tumors, with a range of molecular targets, is becoming more prominent. Technological advancements for PET scanning ensure higher quality imaging and its combination with MRI is especially interesting in pediatric patients. Regarding radionuclides, fluorine-18 is currently strongly preferred because of its beneficial logistics: it has an overall low production cost and its half-life allows for transportation to remote PET centers. Increasingly more studies show superiority of hNET PET ligands like [^{18}F]MFBG and [^{18}F]FDA over [^{123}I]MIBG imaging in terms of diagnostic sensitivity, especially in metastatic disease. Further research on PET ligands and development of imaging modalities will likely lead to improved clinical management of hNET-expressing tumors.

References

1. Tellioglu T,Robertson D. Genetic or acquired deficits in the norepinephrine transporter: current understanding of clinical implications. Expert Rev Mol Med 2001;2001:1-10.

2. Mandela P,Ordway GA. The norepinephrine transporter and its regulation. J Neurochem 2006;97(2):310-33.

3. Pandit-Taskar N,Modak S. Norepinephrine transporter as a target for imaging and therapy. J Nucl Med 2017;58(Suppl 2):39S-53S.

4. Wieland DM, Wu J, Brown LE, Mangner TJ, Swanson DP,Beierwaltes WH. Radiolabeled adrenergic neuron-blocking agents: adrenomedullary imaging with [131I]iodobenzylguanidine. J Nucl Med 1980;21(4):349-53.

5. Bar-Sever Z, Biassoni L, Shulkin B, Kong G, Hofman MS, Lopci E *et al.* Guidelines on nuclear medicine imaging in neuroblastoma. Eur J Nucl Med Mol Imaging 2018;45(11):2009-24.

6. Zhang H, Huang R, Cheung NK, Guo H, Zanzonico PB, Thaler HT *et al.* Imaging the norepinephrine transporter in neuroblastoma: a comparison of [18F]-MFBG and 123I-MIBG. Clin Cancer Res 2014;20(8):2182-91.

7. Zhang H, Huang R, Pillarsetty N, Thorek DLJ, Vaidyanathan G, Serganova I *et al.* Synthesis and evaluation of 18F-labeled benzylguanidine analogs for targeting the human norepinephrine transporter. Eur J Nucl Med Mol Imaging 2014;41(2):322-32.

8. Feldman JM, Blinder RA, Lucas KJ,Coleman RE. Iodine-131 metaiodobenzylguanidine scintigraphy of carcinoid tumors. J Nucl Med 1986;27(11):1691-6.

9. Hanson MW, Feldman JM, Blinder RA, Moore JO,Coleman RE. Carcinoid tumors: iodine-131 MIBG scintigraphy. Radiology 1989;172(3):699-703.

10. Von Moll L, McEwan AJ, Shapiro B, Sisson JC, Gross MD, Lloyd R *et al.* Iodine-131 MIBG scintigraphy of neuroendocrine tumors other than pheochromocytoma and neuroblastoma. J Nucl Med 1987;28(6):979-88.

11. Sundin A, Arnold R, Baudin E, Cwikla JB, Eriksson B, Fanti S *et al.* ENETS consensus guidelines for the standards of care in neuroendocrine tumors: radiological, nuclear medicine & hybrid imaging. Neuroendocrinology 2017;105(3):212-44.

12. Giovanella L, Treglia G, Iakovou I, Mihailovic J, Verburg FA,Luster M. EANM practice guideline for PET/CT imaging in medullary thyroid carcinoma. Eur J Nucl Med Mol Imaging 2020;47(1):61-77.

13. Maguire LH, Thomas AR,Goldstein AM. Tumors of the neural crest: common themes in development and cancer. Dev Dyn 2015;244(3):311-22.

14. Steliarova-Foucher E, Colombet M, Ries LAG, Moreno F, Dolya A, Bray F *et al.* International incidence of childhood cancer, 2001-10: a population-based registry study. Lancet Oncol 2017;18(6):719-31.

15. Maris JM. Recent advances in neuroblastoma. N Engl J Med 2010;362(23):2202-11.

16. Matthay KK, Maris JM, Schleiermacher G, Nakagawara A, Mackall CL, Diller L *et al.* Neuroblastoma. Nat Rev Dis Primers 2016;2:16078.

17. Pinto NR, Applebaum MA, Volchenboum SL, Matthay KK, London WB, Ambros PF *et al.* Advances in risk classification and treatment strategies for neuroblastoma. J Clin Oncol 2015;33(27):3008-17.

18. Brodeur GM. Spontaneous regression of neuroblastoma. Cell Tissue Res 2018;372(2):277-86.

19. Dubois SG, Geier E, Batra V, Yee SW, Neuhaus J, Segal M *et al.* Evaluation of norepinephrine transporter expression and metaiodobenzylguanidine avidity in neuroblastoma: a report from the Children's Oncology Group. Int J Mol Imaging 2012;2012:250834.

20. Streby KA, Shah N, Ranalli MA, Kunkler A,Cripe TP. Nothing but NET: a review of norepinephrine transporter expression and efficacy of 131I-mIBG therapy. Pediatr Blood Cancer 2015;62(1):5-11.

21. Berends AMA, Buitenwerf E, de Krijger RR, Veeger N, van der Horst-Schrivers ANA, Links TP *et al.* Incidence of pheochromocytoma and sympathetic paraganglioma in the Netherlands: a nationwide study and systematic review. Eur J Intern Med 2018.

22. Kiernan CM,Solorzano CC. Pheochromocytoma and Paraganglioma: Diagnosis, Genetics, and Treatment. Surg Oncol Clin N Am 2016;25(1):119-38.

23. Neumann HPH, Young WF, Jr.,Eng C. Pheochromocytoma and Paraganglioma. N Engl J Med 2019;381(6):552-65.

24. Crona J, Taieb D,Pacak K. New perspectives on pheochromocytoma and paraganglioma: toward a molecular classification. Endocr Rev 2017;38(6):489-515.

25. Taieb D, Hicks RJ, Hindie E, Guillet BA, Avram A, Ghedini P *et al.* European Association of Nuclear Medicine Practice Guideline/Society of Nuclear Medicine and Molecular Imaging Procedure Standard 2019 for radionuclide imaging of phaeochromocytoma and paraganglioma. Eur J Nucl Med Mol Imaging 2019;46(10):2112-37.

26. Bruss M, Kunz J, Lingen B,Bonisch H. Chromosomal mapping of the human gene for the tricyclic antidepressant-sensitive noradrenaline transporter. Hum Genet 1993;91(3):278-80.

27. Porzgen P, Bonisch H,Bruss M. Molecular cloning and organization of the coding region of the human norepinephrine transporter gene. Biochem Biophys Res Commun 1995;215(3):1145-50.

28. Meyer J, Wiedemann P, Okladnova O, Bruss M, Staab T, Stober G *et al.* Cloning and functional characterization of the human norepinephrine transporter gene promoter. J Neural Transm 1998;105(10-12):1341-50.

29. Goral I, Latka K,Bajda M. Structure modeling of the norepinephrine transporter. Biomolecules 2020;10(1).

30. Bomanji J, Levison DA, Flatman WD, Horne T, Bouloux PM, Ross G *et al.* Uptake of iodine-123 MIBG by pheochromocytomas, paragangliomas, and neuroblastomas: a histopathological comparison. J Nucl Med 1987;28(6):973-8.

31. Lee KH, Ko BH, Paik JY, Jung KH, Bae JS, Choi JY *et al.* Characteristics and regulation of 123I-MIBG transport in cultured pulmonary endothelial cells. J Nucl Med 2006;47(3):437-42.

32. Armour A, Mairs RJ, Gaze MN,Wheldon TE. Modification of meta-iodobenzylguanidine uptake in neuroblastoma cells by elevated temperature. Br J Cancer 1994;70(3):445-8.

33. Jacobson AF,Travin MI. Impact of medications on mIBG uptake, with specific attention to the heart: Comprehensive review of the literature. J Nucl Cardiol 2015;22(5):980-93.

34. Eisenhofer G. The role of neuronal and extraneuronal plasma membrane transporters in the inactivation of peripheral catecholamines. Pharmacol Ther 2001;91(1):35-62.

35. Iversen LL. Role of transmitter uptake mechanisms in synaptic neurotransmission. Br J Pharmacol 1971;41(4):571-91.

36. Kolby L, Bernhardt P, Levin-Jakobsen AM, Johanson V, Wangberg B, Ahlman H *et al.* Uptake of meta-iodobenzylguanidine in neuroendocrine tumours is mediated by vesicular monoamine transporters. Br J Cancer 2003;89(7):1383-8.

37. Anton M, Wagner B, Haubner R, Bodenstein C, Essien BE, Bonisch H *et al.* Use of the norepinephrine transporter as a reporter gene for non-invasive imaging of genetically modified cells. J Gene Med 2004;6(1):119-26.

38. Smets LA, Janssen M, Metwally E,Loesberg C. Extragranular storage of the neuron blocking agent meta-iodobenzylguanidine (MIBG) in human neuroblastoma cells. Biochem Pharmacol 1990;39(12):1959-64.

39. Wilson JS, Gains JE, Moroz V, Wheatley K,Gaze MN. A systematic review of 131I-meta iodobenzylguanidine molecular radiotherapy for neuroblastoma. Eur J Cancer 2014;50(4):801-15.

40. Bayer M, Kuci Z, Schomig E, Grundemann D, Dittmann H, Handgretinger R *et al.* Uptake of mIBG and catecholamines in noradrenaline- and organic cation transporter-expressing cells: potential use of corticosterone for a preferred uptake in neuroblastoma- and pheochromocytoma cells. Nucl Med Biol 2009;36(3):287-94.

41. Bayer M, Schmitt J, Dittmann H, Handgretinger R, Bruchelt G,Sauter AW. Improved selectivity of mIBG uptake into neuroblastoma cells in vitro and in vivo by inhibition of organic cation transporter 3 uptake using clinically approved corticosteroids. Nucl Med Biol 2016;43(9):543-51.

42. Luzon-Toro B, Geerlings A,Hilfiker S. Hydroxytyrosol increases norepinephrine transporter function in pheochromocytoma cells. Nucl Med Biol 2008;35(7):801-4.

43. More SS, Itsara M, Yang X, Geier EG, Tadano MK, Seo Y *et al.* Vorinostat increases expression of functional norepinephrine transporter in neuroblastoma in vitro and in vivo model systems. Clin Cancer Res 2011;17(8):2339-49.

44. DuBois SG, Groshen S, Park JR, Haas-Kogan DA, Yang X, Geier E *et al.* Phase I study of vorinostat as a radiation qensitizer with 131I-metaiodobenzylguanidine (131I-MIBG) for patients with relapsed or refractory neuroblastoma. Clin Cancer Res 2015;21(12):2715-21.

45. Cleary S,Phillips JK. The norepinephrine transporter and pheochromocytoma. Ann N Y Acad Sci 2006;1073:263-9.

46. Mueller S, Yang X, Sottero TL, Gragg A, Prasad G, Polley MY *et al.* Cooperation of the HDAC inhibitor vorinostat and radiation in metastatic neuroblastoma: efficacy and underlying mechanisms. Cancer Lett 2011;306(2):223-9.

47. McCluskey AG, Boyd M, Ross SC, Cosimo E, Clark AM, Angerson WJ *et al.* [131I]meta-iodobenzylguanidine and topotecan combination treatment of tumors expressing the noradrenaline transporter. Clin Cancer Res 2005;11(21):7929-37.

48. Genolla J, Rodriguez T, Minguez P, Lopez-Almaraz R, Llorens V,Echebarria A. Dosimetry-based high-activity therapy with 131I-metaiodobenzylguanidine (131I-mIBG) and topotecan for the treatment of high-risk refractory neuroblastoma. Eur J Nucl Med Mol Imaging 2019;46(7):1567-75.

49. Bombardieri E, Giammarile F, Aktolun C, Baum RP, Bischof Delaloye A, Maffioli L *et al.* 131I/123I-metaiodobenzylguanidine (mIBG) scintigraphy: procedure guidelines for tumour imaging. Eur J Nucl Med Mol Imaging 2010;37(12):2436-46.

50. Khafagi FA, Shapiro B, Fig LM, Mallette S,Sisson JC. Labetalol reduces iodine-131 MIBG uptake by pheochromocytoma and normal tissues. J Nucl Med 1989;30(4):481-9.

51. Kang JH,Chung JK. Molecular-genetic imaging based on reporter gene expression. J Nucl Med 2008;49 Suppl 2:164S-79S.

52. Brader P, Kelly KJ, Chen N, Yu YA, Zhang Q, Zanzonico P *et al.* Imaging a genetically engineered oncolytic vaccinia virus (GLV-1h99) using a human norepinephrine transporter reporter gene. Clin Cancer Res 2009;15(11):3791-801.

53. Moroz MA, Serganova I, Zanzonico P, Ageyeva L, Beresten T, Dyomina E *et al.* Imaging hNET reporter gene expression with 124I-MIBG. J Nucl Med 2007;48(5):827-36.

54. Neyrinck K, Breuls N, Holvoet B, Oosterlinck W, Wolfs E, Vanbilloen H *et al.* The human somatostatin receptor type 2 as an imaging and suicide reporter gene for pluripotent stem cell-derived therapy of myocardial infarction. Theranostics 2018;8(10):2799-813.

55. Shaikh FA, Kurtys E, Kubassova O,Roettger D. Reporter gene imaging and its role in imaging-based drug development. Drug Discov Today 2020;25(3):582-92.

56. Sisson JC, Frager MS, Valk TW, Gross MD, Swanson DP, Wieland DM *et al.* Scintigraphic localization of pheochromocytoma. N Engl J Med 1981;305(1):12-7.

57. Geatti O, Shapiro B, Sisson JC, Hutchinson RJ, Mallette S, Eyre P *et al.* Iodine-131 metaiodobenzylguanidine scintigraphy for the location of neuroblastoma: preliminary experience in ten cases. J Nucl Med 1985;26(7):736-42.

58. Giammarile F, Chiti A, Lassmann M, Brans B,Flux G. EANM procedure guidelines for 131I-meta-iodobenzylguanidine (131I-mIBG) therapy. Eur J Nucl Med Mol Imaging 2008;35(5):1039-47.

59. Rufini V, Treglia G, Perotti G,Giordano A. The evolution in the use of MIBG scintigraphy in pheochromocytomas and paragangliomas. Hormones 2013;12(1):58-68.

60. Taieb D, Neumann H, Rubello D, Al-Nahhas A, Guillet B,Hindie E. Modern nuclear imaging for paragangliomas: beyond SPECT. J Nucl Med 2012;53(2):264-74.

61. Vallabhajosula S,Nikolopoulou A. Radioiodinated metaiodobenzylguanidine (MIBG): radiochemistry, biology, and pharmacology. Semin Nucl Med 2011;41(5):324-33.

62. Vik TA, Pfluger T, Kadota R, Castel V, Tulchinsky M, Farto JC *et al.* 123I-mIBG scintigraphy in patients with known or suspected neuroblastoma: Results from a prospective multicenter trial. Pediatr Blood Cancer 2009;52(7):784-90.

63. Wiseman GA, Pacak K, O'Dorisio MS, Neumann DR, Waxman AD, Mankoff DA *et al.* Usefulness of 123I-MIBG scintigraphy in the evaluation of patients with known or suspected primary or metastatic pheochromocytoma or paraganglioma: results from a prospective multicenter trial. J Nucl Med 2009;50(9):1448-54.

64. Van Der Horst-Schrivers AN, Jager PL, Boezen HM, Schouten JP, Kema IP,Links TP. Iodine-123 metaiodobenzylguanidine scintigraphy in localising phaeochromocytomas--experience and meta-analysis. Anticancer Res 2006;26(2B):1599-604.

65. Xia J, Zhang H, Hu Q, Liu SY, Zhang LQ, Zhang A *et al.* Comparison of diagnosing and staging accuracy of PET (CT) and MIBG on patients with neuroblastoma: Systemic review and meta-analysis. J Huazhong Univ Sci Technolog Med Sci 2017;37(5):649-60.

66. Timmers HJ, Chen CC, Carrasquillo JA, Whatley M, Ling A, Havekes B *et al.* Comparison of 18F-fluoro-L-DOPA, 18F-fluoro-deoxyglucose, and 18F-fluorodopamine PET and 123I-MIBG scintigraphy in the localization of pheochromocytoma and paraganglioma. J Clin Endocrinol Metab 2009;94(12):4757-67.

67. Timmers HJ, Eisenhofer G, Carrasquillo JA, Chen CC, Whatley M, Ling A *et al.* Use of 6-[18F]-fluorodopamine positron emission tomography (PET) as first-line investigation for the diagnosis and localization of non-metastatic and metastatic phaeochromocytoma (PHEO). Clin Endocrinol (Oxf) 2009;71(1):11-7.

68. Fiebrich HB, Brouwers AH, Kerstens MN, Pijl ME, Kema IP, de Jong JR *et al.* 6-[F-18]Fluoro-L-dihydroxyphenylalanine positron emission tomography is superior to conventional imaging with 123I-metaiodobenzylguanidine scintigraphy, computer tomography, and magnetic resonance imaging in localizing tumors causing catecholamine excess. J Clin Endocrinol Metab 2009;94(10):3922-30.

69. Ilias I, Chen CC, Carrasquillo JA, Whatley M, Ling A, Lazurova I *et al.* Comparison of 6-18F-fluorodopamine PET with 123I-metaiodobenzylguanidine and 111in-pentetreotide scintigraphy in localization of nonmetastatic and metastatic pheochromocytoma. J Nucl Med 2008;49(10):1613-9.

70. Timmers HJ, Kozupa A, Chen CC, Carrasquillo JA, Ling A, Eisenhofer G *et al.* Superiority of fluorodeoxyglucose positron emission tomography to other functional imaging

techniques in the evaluation of metastatic SDHB-associated pheochromocytoma and paraganglioma. J Clin Oncol 2007;25(16):2262-9.

71. Fonte JS, Robles JF, Chen CC, Reynolds J, Whatley M, Ling A *et al.* False-negative 123I-MIBG SPECT is most commonly found in SDHB-related pheochromocytoma or paraganglioma with high frequency to develop metastatic disease. Endocr Relat Cancer 2012;19(1):83-93.

72. Taieb D, Tessonnier L, Sebag F, Niccoli-Sire P, Morange I, Colavolpe C *et al.* The role of 18F-FDOPA and 18F-FDG-PET in the management of malignant and multifocal phaeochromocytomas. Clin Endocrinol (Oxf) 2008;69(4):580-6.

73. King KS, Chen CC, Alexopoulos DK, Whatley MA, Reynolds JC, Patronas N *et al.* Functional imaging of SDHx-related head and neck paragangliomas: comparison of 18F-fluorodihydroxyphenylalanine, 18F-fluorodopamine, 18F-fluoro-2-deoxy-D-glucose PET, 123I-metaiodobenzylguanidine scintigraphy, and 111In-pentetreotide scintigraphy. J Clin Endocrinol Metab 2011;96(9):2779-85.

74. Janssen I, Chen CC, Taieb D, Patronas NJ, Millo CM, Adams KT *et al.* 68Ga-DOTATATE PET/CT in the Localization of Head and Neck Paragangliomas Compared with Other Functional Imaging Modalities and CT/MRI. J Nucl Med 2016;57(2):186-91.

75. Ady N, Zucker JM, Asselain B, Edeline V, Bonnin F, Michon J *et al.* A new 123I-MIBG whole body scan scoring method--application to the prediction of the response of metastases to induction chemotherapy in stage IV neuroblastoma. Eur J Cancer 1995;31A(2):256-61.

76. Lewington V, Lambert B, Poetschger U, Sever ZB, Giammarile F, McEwan AJB *et al.* 123I-mIBG scintigraphy in neuroblastoma: development of a SIOPEN semi-quantitative reporting ,method by an international panel. Eur J Nucl Med Mol Imaging 2017;44(2):234-41.

77. Matthay KK, Edeline V, Lumbroso J, Tanguy ML, Asselain B, Zucker JM *et al.* Correlation of early metastatic response by 123I-metaiodobenzylguanidine scintigraphy with

overall response and event-free survival in stage IV neuroblastoma. J Clin Oncol 2003;21(13):2486-91.

78. Yanik GA, Parisi MT, Shulkin BL, Naranjo A, Kreissman SG, London WB *et al.* Semiquantitative mIBG scoring as a prognostic indicator in patients with stage 4 neuroblastoma: a report from the Children's oncology group. J Nucl Med 2013;54(4):541-8.

79. Decarolis B, Schneider C, Hero B, Simon T, Volland R, Roels F *et al.* Iodine-123 metaiodobenzylguanidine scintigraphy scoring allows prediction of outcome in patients with stage 4 neuroblastoma: results of the Cologne interscore comparison study. J Clin Oncol 2013;31(7):944-51.

80. Cistaro A, Quartuccio N, Caobelli F, Piccardo A, Paratore R, Coppolino P *et al.* 124I-MIBG: a new promising positron-emitting radiopharmaceutical for the evaluation of neuroblastoma. Nucl Med Rev Cent East Eur 2015;18(2):102-6.

81. Hartung-Knemeyer V, Rosenbaum-Krumme S, Buchbender C, Poppel T, Brandau W, Jentzen W *et al.* Malignant pheochromocytoma imaging with [124I]mIBG PET/MR. J Clin Endocrinol Metab 2012;97(11):3833-4.

82. Huang SY, Bolch WE, Lee C, Van Brocklin HF, Pampaloni MH, Hawkins RA *et al.* Patient-specific dosimetry using pretherapy [124I]m-iodobenzylguanidine ([124I]mIBG) dynamic PET/CT imaging before [131I]mIBG targeted radionuclide therapy for neuroblastoma. Mol Imaging Biol 2015;17(2):284-94.

83. Ott RJ, Tait D, Flower MA, Babich JW,Lambrecht RM. Treatment planning for 131I-mIBG radiotherapy of neural crest tumours using 124I-mIBG positron emission tomography. Br J Radiol 1992;65(777):787-91.

84. Seo Y, Huh Y, Huang SY, Hernandez-Pampaloni JM, Hawkins RA, Gustafson WC *et al.* Technical Note: Simplified and practical pretherapy tumor dosimetry - A feasibility study

for (131) I-MIBG therapy of neuroblastoma using (124) I-MIBG PET/CT. Med Phys 2019;46(5):2477-86.

85. Garg PK, Garg S,Zalutsky MR. Synthesis and preliminary evaluation of para- and meta-[18F]fluorobenzylguanidine. Nucl Med Biol 1994;21(1):97-103.

86. Pauwels E, Cleeren F, Bormans G,Deroose CM. Somatostatin receptor PET ligands - the next generation for clinical practice. Am J Nucl Med Mol Imaging 2018;8(5):311-31.

87. Hu B, Vāvere AL, Neumann KD, Shulkin BL, DiMagno SG,Snyder SE. A practical, automated synthesis of meta-[18F]fluorobenzylguanidine for clinical use. ACS Chem Neurosci 2015;6(11):1870-9.

88. Rotstein BH, Wang L, Liu RY, Patteson J, Kwan EE, Vasdev N *et al.* Mechanistic studies and radiofluorination of structurally diverse pharmaceuticals with spirocyclic iodonium(III) ylides. Chem Sci 2016;7(7):4407-17.

89. Pandit-Taskar N, Zanzonico P, Staton KD, Carrasquillo JA, Reidy-Lagunes D, Lyashchenko S *et al.* Biodistribution and dosimetry of 18F-meta-fluorobenzylguanidine: a first-in-human PET/CT imaging study of patients with neuroendocrine malignancies. J Nucl Med 2018;59(1):147-53.

90. Pauwels E, Celen S, Vandamme M, Leysen W, Baete K, Bechter O *et al.* Improved resolution and sensitivity of [18F]MFBG PET compared with [123I]MIBG SPECT in a patient with a norepinephrine transporter–expressing tumour. Eur J Nucl Med Mol Imaging 2020 May 8 [Epub ahead of print]. doi:10.1007/s00259-020-04830-x.

91. Boschi S, Lodi F, Boschi L, Nanni C, Chondrogiannis S, Colletti PM *et al.* 11C-meta-hydroxyephedrine: a promising PET radiopharmaceutical for imaging the sympathetic nervous system. Clin Nucl Med 2015;40(2):e96-e103.

92. Franzius C, Hermann K, Weckesser M, Kopka K, Juergens KU, Vormoor J *et al.* Whole-body PET/CT with 11C-meta-hydroxyephedrine in tumors of the sympathetic nervous system:

feasibility study and comparison with 123I-MIBG SPECT/CT. J Nucl Med 2006;47(10):1635-42.

93. Mann GN, Link JM, Pham P, Pickett CA, Byrd DR, Kinahan PE *et al.* [11C]metahydroxyephedrine and [18F]fluorodeoxyglucose positron emission tomography improve clinical decision making in suspected pheochromocytoma. Ann Surg Oncol 2006;13(2):187-97.

94. Shulkin BL, Wieland DM, Baro ME, Ungar DR, Mitchell DS, Dole MG *et al.* PET hydroxyephedrine imaging of neuroblastoma. J Nucl Med 1996;37(1):16-21.

95. Shulkin BL, Wieland DM, Schwaiger M, Thompson NW, Francis IR, Haka MS *et al.* PET scanning with hydroxyephedrine: an approach to the localization of pheochromocytoma. J Nucl Med 1992;33(6):1125-31.

96. Trampal C, Engler H, Juhlin C, Bergstrom M,Langstrom B. Pheochromocytomas: detection with 11C hydroxyephedrine PET. Radiology 2004;230(2):423-8.

97. Yamamoto S, Hellman P, Wassberg C,Sundin A. 11C-hydroxyephedrine positron emission tomography imaging of pheochromocytoma: a single center experience over 11 years. J Clin Endocrinol Metab 2012;97(7):2423-32.

98. Pacak K, Eisenhofer G, Carrasquillo JA, Chen CC, Li ST,Goldstein DS. 6-[18F]fluorodopamine positron emission tomographic (PET) scanning for diagnostic localization of pheochromocytoma. Hypertension 2001;38(1):6-8.

99. Ilias I, Yu J, Carrasquillo JA, Chen CC, Eisenhofer G, Whatley M *et al.* Superiority of 6-[18F]-fluorodopamine positron emission tomography versus [131I]-metaiodobenzylguanidine scintigraphy in the localization of metastatic pheochromocytoma. J Clin Endocrinol Metab 2003;88(9):4083-7.

100. Kaji P, Carrasquillo JA, Linehan WM, Chen CC, Eisenhofer G, Pinto PA *et al.* The role of 6-[18F]fluorodopamine positron emission tomography in the localization of adrenal

pheochromocytoma associated with von Hippel-Lindau syndrome. Eur J Endocrinol 2007;156(4):483-7.

101. Zelinka T, Timmers HJ, Kozupa A, Chen CC, Carrasquillo JA, Reynolds JC *et al.* Role of positron emission tomography and bone scintigraphy in the evaluation of bone involvement in metastatic pheochromocytoma and paraganglioma: specific implications for succinate dehydrogenase enzyme subunit B gene mutations. Endocr Relat Cancer 2008;15(1):311-23.

102. Suh M, Park HJ, Choi HS, So Y, Lee BC,Lee WW. Case report of PET/CT imaging of a patient with neuroblastoma using 18F-FPBG. Pediatrics 2014;134(6):e1731-4.

103. Lokitz SJ, Garg S, Nazih R,Garg PK. Whole body PET imaging with a norepinephrine transporter probe 4-[18F]fluorobenzylguanidine: biodistribution and radiation dosimetry. Mol Imaging Biol 2019;21(4):686-95.

104. Vaidyanathan G, Affleck DJ,Zalutsky MR. (4-[18F]fluoro-3-iodobenzyl)guanidine, a potential MIBG analogue for positron emission tomography. J Med Chem 1994;37(21):3655-62.

105. Vaidyanathan G, Affleck DJ,Zalutsky MR. Validation of 4-[fluorine-18]fluoro-3-iodobenzylguanidine as a positron-emitting analog of MIBG. J Nucl Med 1995;36(4):644-50.

106. Yamaguchi A, Hanaoka H, Higuchi T,Tsushima Y. Radiolabeled (4-Fluoro-3-Iodobenzyl)Guanidine Improves Imaging and Targeted Radionuclide Therapy of Norepinephrine Transporter-Expressing Tumors. J Nucl Med 2018;59(5):815-21.

107. Sinusas AJ, Lazewatsky J, Brunetti J, Heller G, Srivastava A, Liu YH *et al.* Biodistribution and radiation dosimetry of LMI1195: first-in-human study of a novel 18F-labeled tracer for imaging myocardial innervation. J Nucl Med 2014;55(9):1445-51.

108. Gaertner FC, Wiedemann T, Yousefi BH, Lee M, Repokis I, Higuchi T *et al.* Preclinical evaluation of 18F-LMI1195 for in vivo imaging of pheochromocytoma in the MENX tumor model. J Nucl Med 2013;54(12):2111-7.

109. Raffel DM, Jung YW, Koeppe RA, Jang KS, Gu G, Scott PJH *et al.* First-in-human studies of [18F] fluorohydroxyphenethylguanidines. Circ Cardiovasc Imaging 2018;11(12):e007965.

110. Treglia G, Cocciolillo F, de Waure C, Di Nardo F, Gualano MR, Castaldi P *et al.* Diagnostic performance of 18F-dihydroxyphenylalanine positron emission tomography in patients with paraganglioma: a meta-analysis. Eur J Nucl Med Mol Imaging 2012;39(7):1144-53.

111. Piccardo A, Lopci E, Conte M, Garaventa A, Foppiani L, Altrinetti V *et al.* Comparison of 18F-dopa PET/CT and 123I-MIBG scintigraphy in stage 3 and 4 neuroblastoma: a pilot study. Eur J Nucl Med Mol Imaging 2012;39(1):57-71.

112. Piccardo A, Morana G, Puntoni M, Campora S, Sorrentino S, Zucchetta P *et al.* Diagnosis, Treatment Response, and Prognosis: The Role of (18)F-DOPA PET/CT in Children Affected by Neuroblastoma in Comparison with (123)I-mIBG Scan: The First Prospective Study. J Nucl Med 2020;61(3):367-74.

113. Timmers HJ, Chen CC, Carrasquillo JA, Whatley M, Ling A, Eisenhofer G *et al.* Staging and functional characterization of pheochromocytoma and paraganglioma by 18F-fluorodeoxyglucose (18F-FDG) positron emission tomography. J Natl Cancer Inst 2012;104(9):700-8.

114. van Berkel A, Vriens D, Visser EP, Janssen MJR, Gotthardt M, Hermus A *et al.* Metabolic subtyping of pheochromocytoma and paraganglioma by 18F-FDG pharmacokinetics using dynamic PET/CT scanning. J Nucl Med 2019;60(6):745-51.

115. Han S, Suh CH, Woo S, Kim YJ,Lee JJ. Performance of 68Ga-DOTA-conjugated somatostatin receptor-targeting peptide PET in detection of pheochromocytoma and paraganglioma: a systematic review and metaanalysis. J Nucl Med 2019;60(3):369-76.

Tables:

Table 1: Physical characteristics of the discussed radionuclides. In case of β^- emission, the energy stands for the maximal β^- energy, whereas in case of β^+ emission, it stands for the mean β^+ energy. For β-emitters, the intensity equals the branching ratio. Data from the Laboratoire National Henri Becquerel (http://www.nucleide.org/Laraweb) and Brookhaven National Laboratory (http://www.nndc.bnl.gov/nudat2).

Radionuclide	**Half-life**	**Decay mode**	**Energy (keV)**	**Intensity**	**Daughter nucleus**
iodine-123	13.223 d	100% electron capture			tellurium-123
		excited state emissions (γ)	159.0	83.25%	
iodine-124	4.176 d	22.7% β^+ emission	820.0	22.7%	tellurium-124
		77.3% electron capture			
		excited state emissions (γ)	602.7	62.9%	
iodine-131	8.023 d	100% β^- emission	606.3	89.6%	xenon-131
		excited state emissions (γ)	364.4	81.2%	
fluorine-18	109.8 min	96.73% β^+ emission	249.8	96.73%	oxygen-18
		3.27% electron capture			
carbon-11	20.36 min	99.77% β^+ emission	385.7	99.77%	boron-11
		0.23% electron capture			

Table 2: The (modified) Curie and SIOPEN scoring system for standardized and objective assessment of disease load in neuroblastoma patients and 5-year event-free survival (EFS) and overall survival (OS) according to the optimal cutoff point identified by Decarolis *et al.*[79].

	(modified) Curie score	**SIOPEN score**
Areas of interest	• 9 skeletal • 1 soft tissue	12 skeletal
Score per area	Skeletal: 0. No involvement 1. 1 site of involvement 2. > 1 site of involvement 3. > 50% involvement of area Soft tissue: 0. No involvement 1. 1 soft tissue lesion 2. > 1 soft tissue lesion 3. Soft tissue lesion occupying > 50% of chest or abdomen	0. No abnormality 1. 1 discrete focus 2. 2 discrete foci 3. 3 discrete foci 4. > 3 discrete foci or diffuse involvement < 50% of area 5. Diffuse involvement 50-95% of area 6. Uniform, diffuse involvement of area
Maximum score	30	72
5-year EFS	• ≤ 2: 70% ± 15% • > 2: 27% ± 7%	• ≤ 4: 67% ± 14% • > 4: 26% ± 7%
5-year OS	• ≤ 2: 90% ± 10% • > 2: 42% ± 7%	• ≤ 4: 83% ± 11% • > 4: 41% ± 8%

Titles of figures:

Figure 1: Chemical structures of several discussed molecules: (A) (1R)-norepinephrine, (B) *meta*-[$^{123/124/131}$I]iodobenzylguanidine ([$^{123/124/131}$I]MIBG), (C) *meta*-[^{18}F]fluorobenzylguanidine ([^{18}F]MFBG), (D) *para*-[^{18}F]fluorobenzylguanidine ([^{18}F]PFBG), (E) (1R 2S) *meta*-[^{11}C]hydroxyephedrine ([^{11}C]HED), (F) 6-[^{18}F]fluorodopamine ([^{18}F]FDA).

Figure 2: Mechanisms potentially involved in *meta*-iodobenzylguanidine (MIBG) handling: uptake, storage (in neurosecretory vesicles and mitochondria) and release. hNET: human norepinephrine transporter, VMAT: vesicular monoamine transporter, Na^+/K^+-ATPase: sodium potassium pump, Na^+: sodium, Cl^-: chloride, K^+: potassium.

Figure 3: Head-to-head comparison of [^{123}I]MIBG scintigraphy (A: planar anterior, B: planar posterior, E and G: transversal SPECT/CT images) and [^{18}F]MFBG PET (C: maximum-intensity anterior projection, D: maximum-intensity posterior projection, F and H: transversal PET/CT images) of a 36-year old patient with metastatic paraganglioma (patient data from an ongoing clinical trial, clinicaltrials.gov identifier: NCT04258592). Blue arrows indicate additional bone and lymph node lesions that were visualized with [^{18}F]MFBG.

Figure 1: Chemical structures of several discussed molecules: (A) (1R)-norepinephrine, (B) *meta*-[$^{123/124/131}$I]iodobenzylguanidine ([$^{123/124/131}$I]MIBG), (C) *meta*-[^{18}F]fluorobenzylguanidine ([^{18}F]MFBG), (D) *para*-[^{18}F]fluorobenzylguanidine ([^{18}F]PFBG), (E) (1R 2S) *meta*-[^{11}C]hydroxyephedrine ([^{11}C]HED), (F) 6-[^{18}F]fluorodopamine ([^{18}F]FDA).

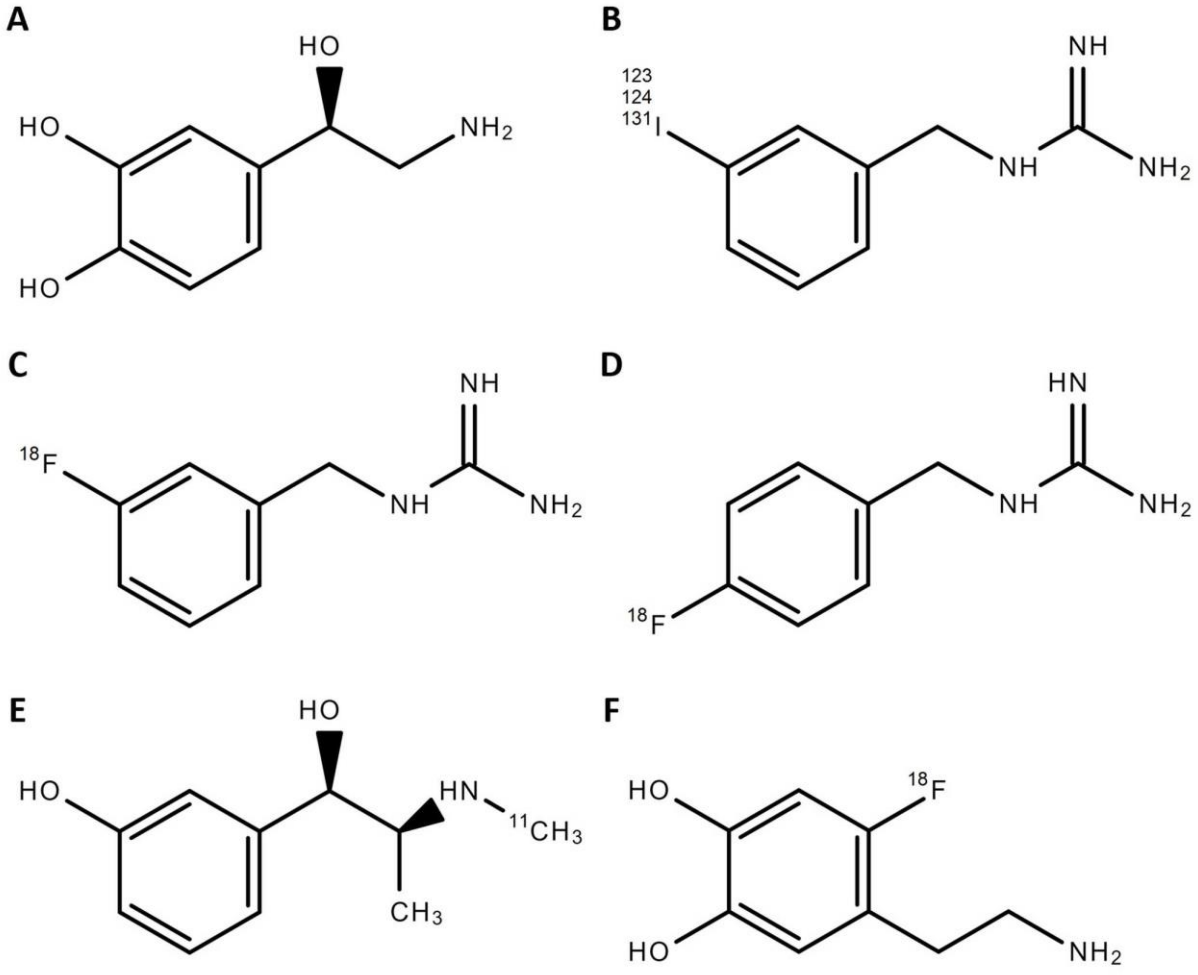

Figure 2: Mechanisms potentially involved in *meta*-iodobenzylguanidine (MIBG) handling: uptake, storage (in neurosecretory vesicles and mitochondria) and release. hNET: human norepinephrine transporter, VMAT: vesicular monoamine transporter, Na^+/K^+-ATPase: sodium potassium pump, Na^+: sodium, Cl^-: chloride, K^+: potassium.

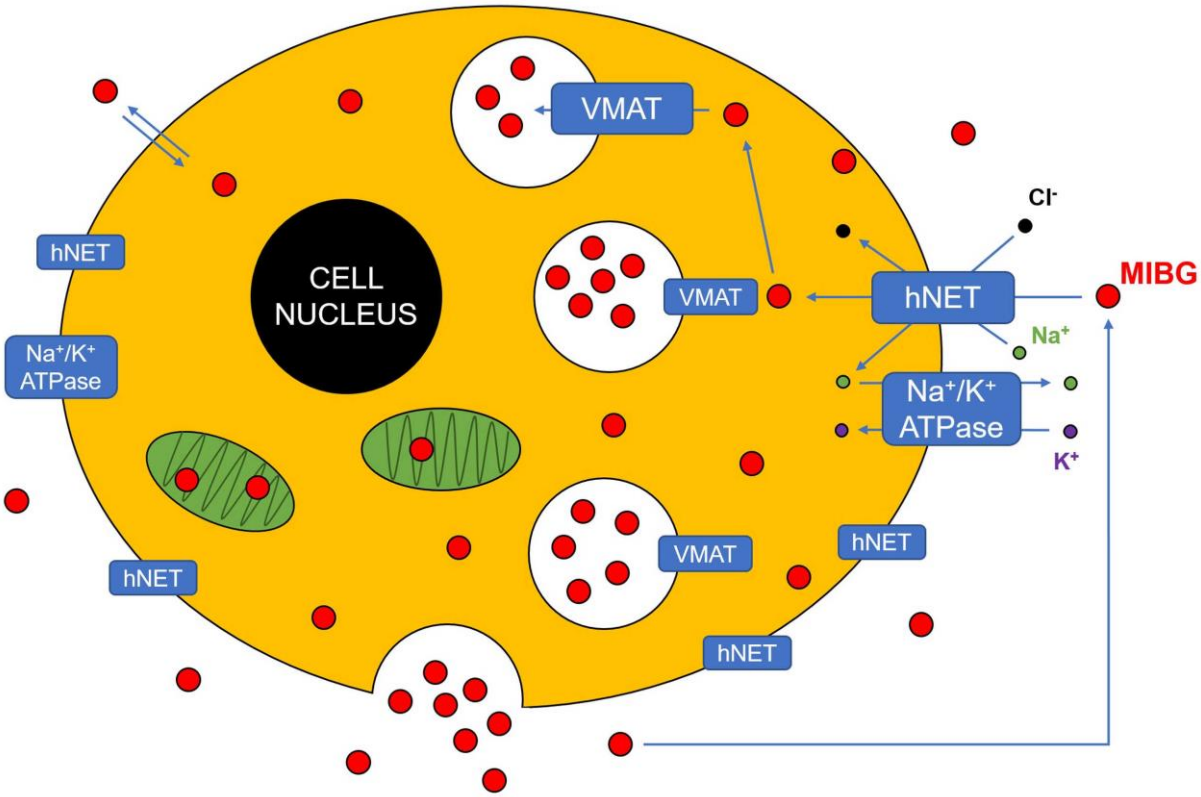

Figure 3: Head-to-head comparison of [^{123}I]MIBG scintigraphy (A: planar anterior, B: planar posterior, E and G: transversal SPECT/CT images) and [^{18}F]MFBG PET (C: maximum-intensity anterior projection, D: maximum-intensity posterior projection, F and H: transversal PET/CT images) of a 36-year old patient with metastatic paraganglioma (patient data from an ongoing clinical trial, clinicaltrials.gov identifier: NCT04258592). Blue arrows indicate additional bone and lymph node lesions that were visualized with [^{18}F]MFBG.